Supporting Information

High performance MBene substrate for improving the MnO_2 cathode of aqueous Zn-ion battery

Shanshan Fan,[a] Zihan Shen,[b] Jiasen Yin,[a] Zhenghua Wang,[a] and Jun Pu[b,*]

[a] *Key Laboratory of Functional Molecular Solids, Ministry of Education, Anhui Provincial Engineering Laboratory for New-Energy Vehicle Battery Energy-Storage Materials, College of Chemistry and Materials Science, Anhui Normal University, Wuhu 241002, China*

[b] *State Key Laboratory of Multiphase Complex Systems, Institute of Process Engineering, Chinese Academy of Sciences, Beijing 100190, China*

* Corresponding author

E-mail: jpu@anhu.edu

Experimental Section

1. Preparation of MoB-based MBene

Typically, 1 g of MoAlB powder was dispersed into NaOH solution with a mass fraction of 25% and stirred by ultrasound. The fully mixed solution was then transferred to a high-pressure hydrothermal reactor where it reacted at 150 °C for 24 h. After the reaction, the samples were repeatedly centrifuged with deionized water and then freeze-dried.

The freeze-dried samples were stripped and stratified. The diluted tetramethylammonium hydroxide solution (TMAOH) solution was stirred for 12 h, and then centrifuged at 4000 rpm by a high-speed centrifuge for 10 min. The remaining TMAOH was removed, washed repeatedly with deionized water and anhydrous ethanol, and finally freeze-dried.

2. In-situ growth of δ-MnO_2 on MBene

A certain amount of $KMnO_4$ (230 mg) and $MnSO_4$ (38 mg) were weighed and dissolved in 20 mL deionized water, respectively. Then, 30 mg as-prepared MoB-based MBene was ultrasonically dispersed in 10 mL deionized water, stirred for 30 min, mixed evenly, transferred to a high-pressure reactor and kept at 160 °C for 12 h. After the hydrothermal reaction, washed and freeze-dried to obtain MoB/MnO_2. Pure MnO_2 was prepared using the same method, except that MBene solution was not added.

3. Materials characterization

Under the Cu Kα radiation at 1.5418 Å, the crystal structure and phase were recorded on X-ray diffractometer (XRD, Rigaku Smart Lab). The morphology was determined by field emission scanning electron microscope at 10 kV(SEM, Hitachi Regulus 8100). The crystal surface parameters were carried out by transmission electron microscope (TEM) and high-resolution TEM (HRTEM) at 200 kV (FEI Talos F200x). The energy-dispersive X-ray spectroscopy elemental mapping was recorded on a Talos F200x device (Thermo Fisher). Infrared spectroscopy (DTGS KBr) was used to measure functional groups on the sample surface. The valence states and chemical information of the sample surface were analyzed by X-ray photoelectron spectroscopy (XPS, Thermo Scientific ESCALAB

Xi+). The N_2 adsorption–desorption isotherms and surface area analyze were measured via Micromeritics ASAP 2460.

4. Electrochemical performance tests

The assembled CR-2032 coin cells were used for electrochemical analysis. First, the active material, acetylene black and polyvinylidene fluoride (PVDF) were ground according to the mass ratio of 7:2:1, and N-methyl pyrrolidone (NMP) was added to form an ink-like slurry, which was coated on graphite paper and vacuum dried at 60 °C with a load greater than 1.0 g cm^{-2}. Meanwhile, metal Zn sheet was used as the anode, 2.0 M $ZnSO_4$ and 0. 2 M $MnSO_4$ mixed solution was the electrolyte, Whatman glass fiber diaphragm was the separator. Finally, the charge-discharge cycle and stability tests were carried out on LAND with a voltage window of 0.8–1.8 V. Cyclic voltammetry (CV) and electrochemical impedance spectroscopy (EIS, frequency range: 10^5–10^{-2} Hz) were tested on the CHI660E electrochemical workstation.

5. Theoretical calculation

The optimize geometries and electronic properties of all the investigated structures in this study were calculated based on Cambridge Sequential Total Energy Package (CASTEP). It was employed with general gradient approximation and Perdew-Burke-Ernzerhof exchange-correlation functional.[1,2] A plane-wave cutoff energy of 500 eV was adopted for the standard norm-conserving pseudopotentials.[3] The Brillouin zone was sampled with Monkhorst−Pack mesh k-points of 2×2×1 grid. A vacuum slab thickness of 15 Å was set between slabs along the Z-axis.

Figures:

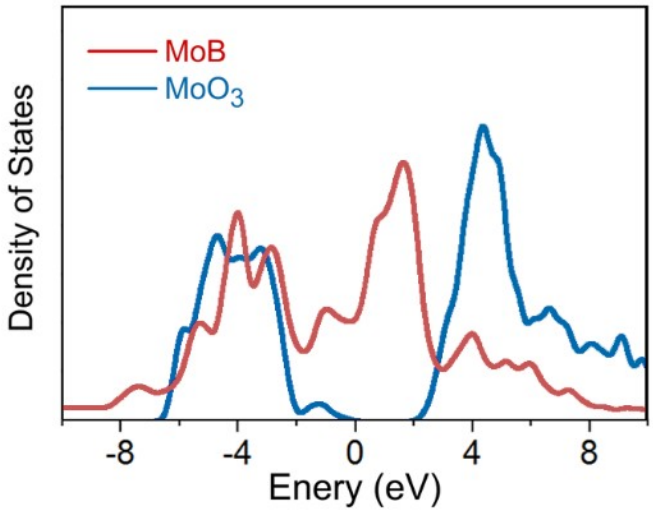

Fig. S1. Density of states results of MoB and MoO_3.

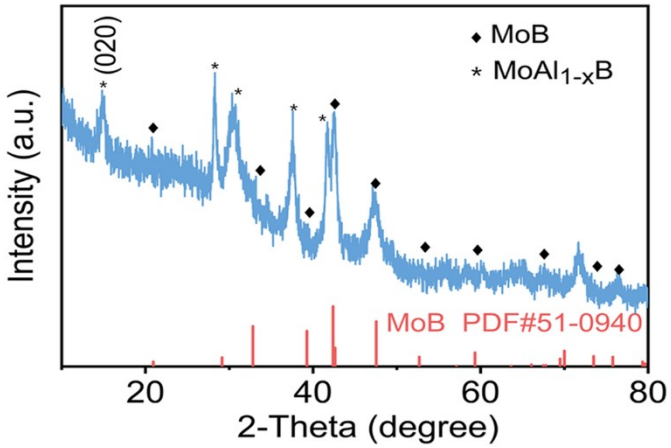

Fig. S2. XRD of as-prepared MoB-based MBene sample.

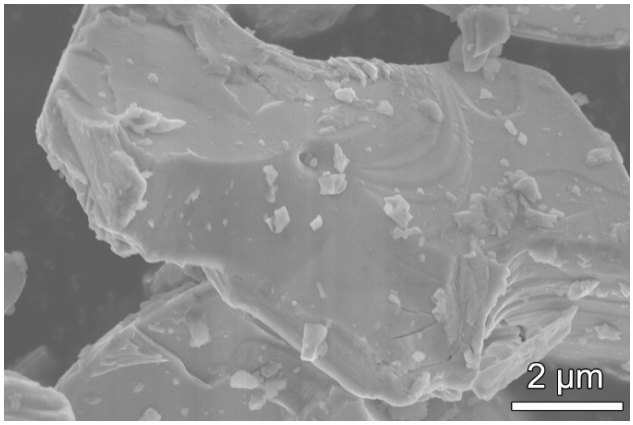

Fig. S3. SEM of initial MoAlB precursor.

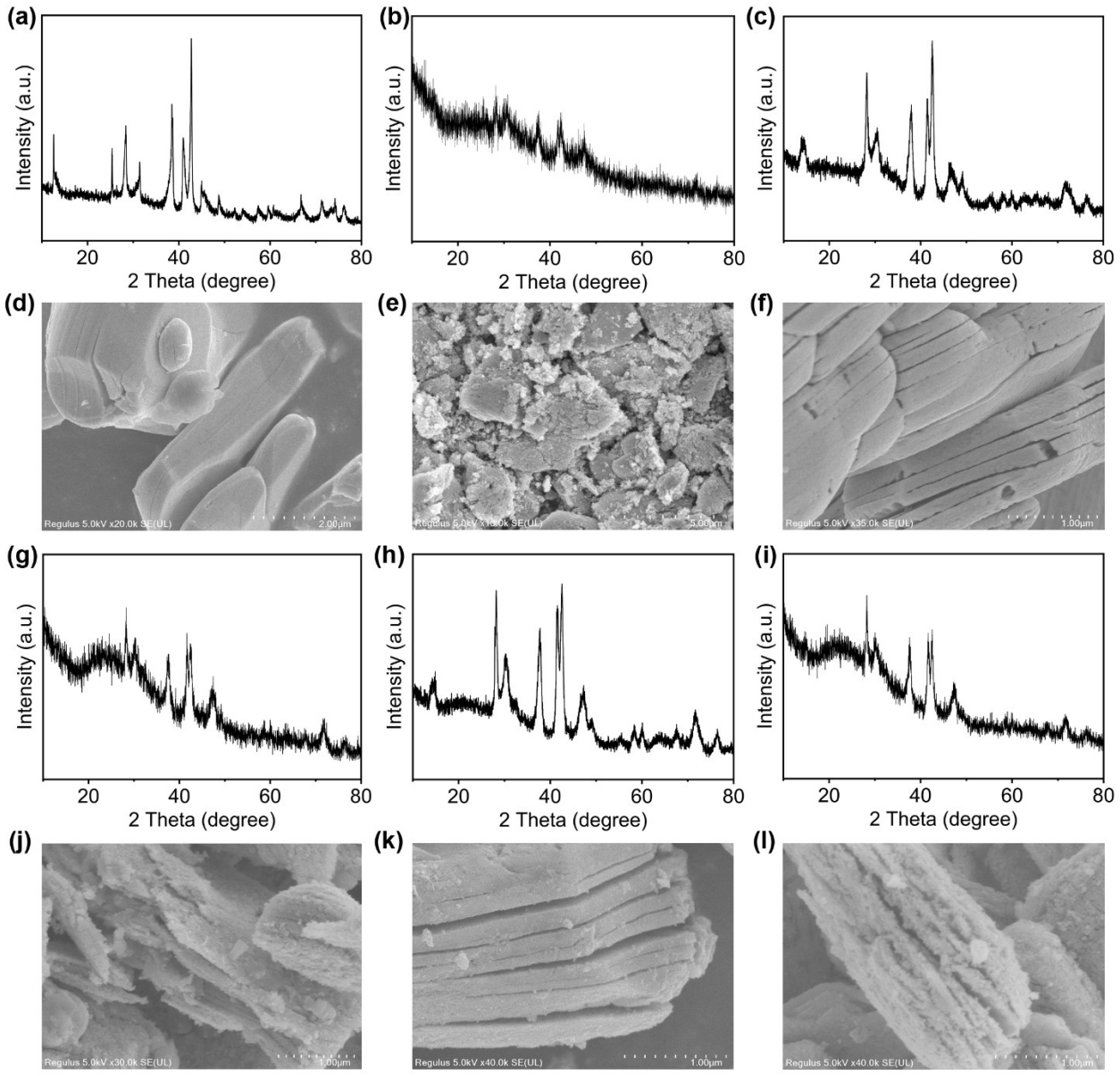

Fig. S4. The influence of different etching conditions on the product. Temperature: (a,d) 25% NaOH, 25 °C for 24 h; (b,e) 25% NaOH, 160 °C for 24 h. Alkali concentration: (c,f) 10% NaOH, 150 °C for 24 h; (g,j) 30% NaOH, 150 °C for 24 h. Time: (h,k) 25% NaOH, 150 °C for 12 h; (i,l) 25% NaOH, 150 °C for 30 h.

Although the Al content might be reduced somewhat, the overall accordion layered structure collapsed, which was not conducive to the MnO_2 payload. Therefore, in order to obtain 2D MBene materials with larger layer spacing and thinner, it was very reasonable and effective to select NaOH with a mass fraction of 25 wt% in the manuscript for etching at 150 °C for 24 h.

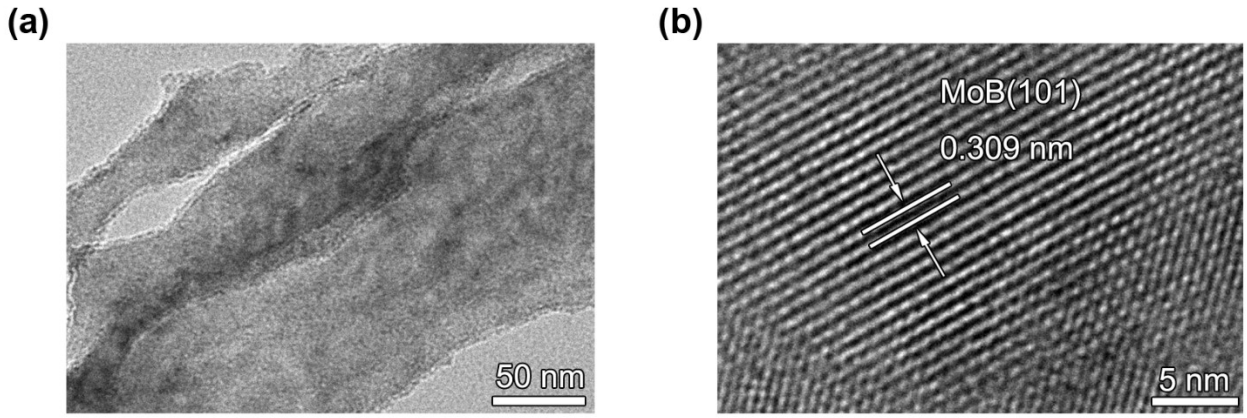

Fig. S5. (a) TEM and (b) HRTEM of MoB nanosheet.

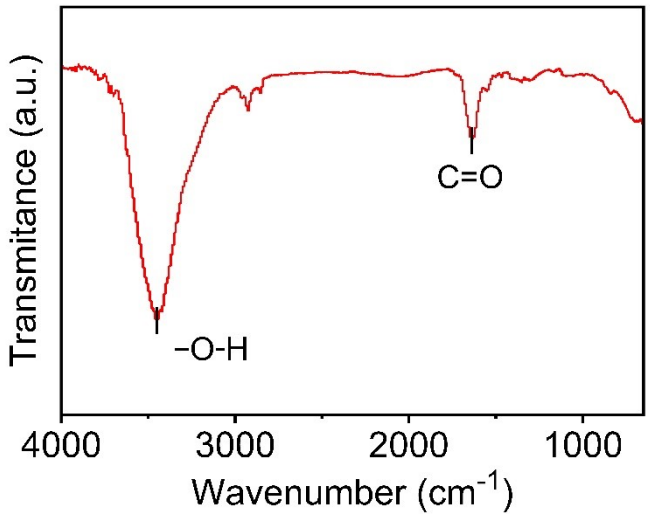

Fig. S6. Infrared spectrum of MoB.

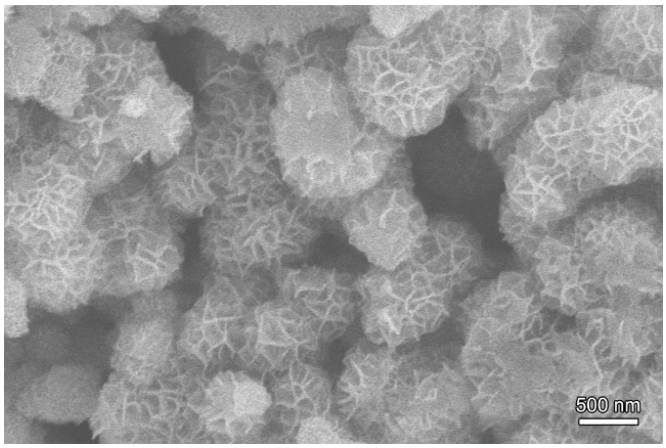

Fig. S7. SEM of pure MnO_2.

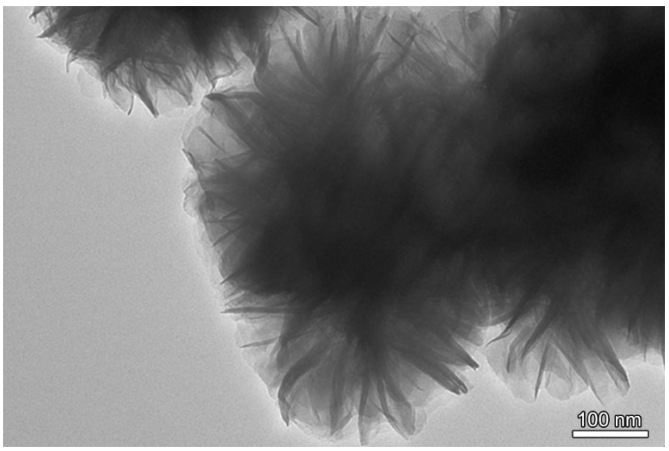

Fig. S8. TEM of pure MnO_2.

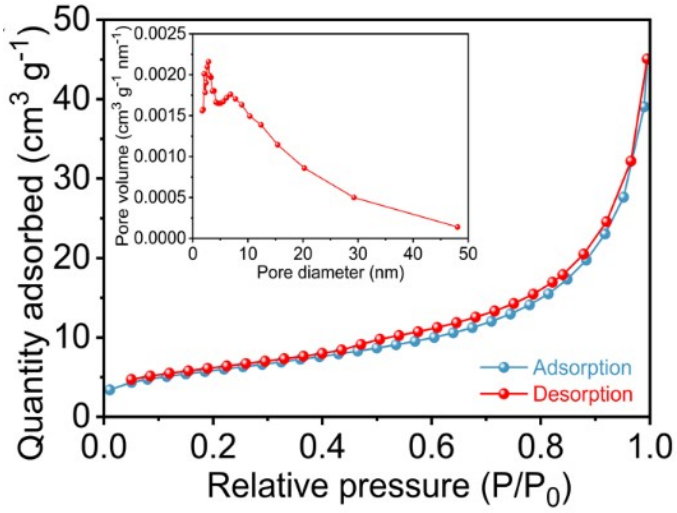

Fig. S9. N_2 adsorption-desorption curve and corresponding pore size distribution.

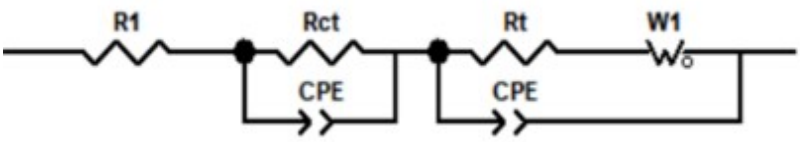

Fig. S10. The equivalent circuit of EIS.

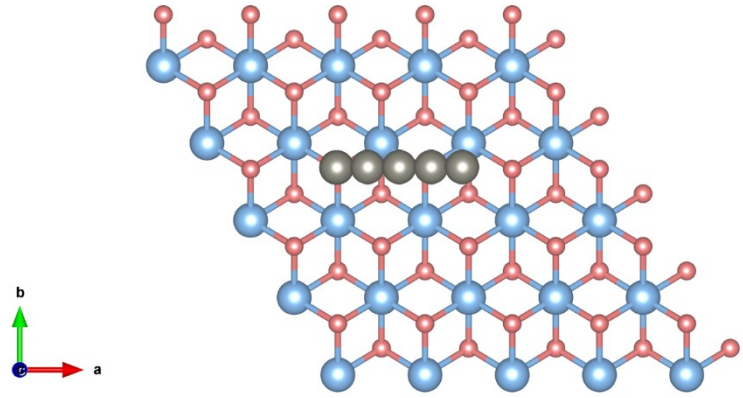

Fig. S11. Diffusion path of Zn-ions on MnO_2 surface.

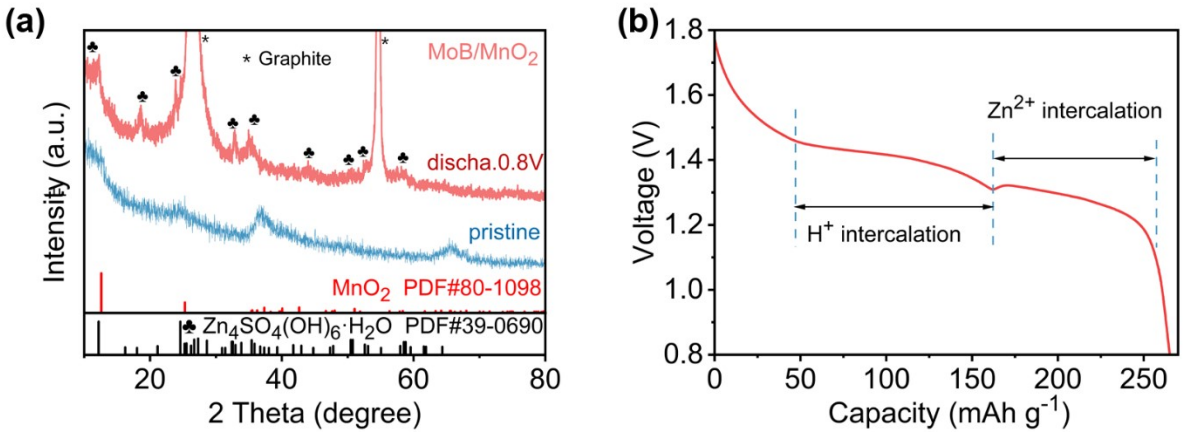

Fig. S12. (a) XRD test of MnO_2 electrode after discharge. (b) The dominant reaction at different voltages.

Table S1. Comparison of this work with other MnO_2 cathodes.

Materials	Capacity (mAh g^{-1})	Capacity retention	Ref.
MnO_2@AEPA	200 (0.3 A g^{-1})	87% (110 cycles)	4
δ-MnO_2	250 (0.2 A g^{-1})	66% (100 cycles)	5
Cu^{2+}-MnO_2	280 (0.2 A g^{-1})	94% (90 cycles)	6
H-MnO_2	100 (0.4 A g^{-1})	98% (100 cycles)	7
CoxMnO_2	105 (0.5 A g^{-1})	84.6% (500 cycles)	8
MnO_2@NG	157 (0.5 A g^{-1})	~100% (500 cycles)	9
δa-MnO_2	175 (0.5 A g^{-1})	~100% (100 cycles)	10
MnHCF	229 (0.1 A g^{-1})	87.1% (100 cycles)	11
CS@Ce-MnO_2	200 (1 A g^{-1})	~60% (2800 cycles)	12
SP@PDA-d-δ-MnO_2	204.8 (1 A g^{-1})	35.8% (500 cycles)	13
MnN	200 (1 A g^{-1})	69% (1000 cycles)	14
δ-MnO_2	221 (0.5 A g^{-1})	~100% (100 cycles)	15
MoB/MnO_2	264.9 (0.2 A g^{-1})	94% (50 cycles)	This work
	232.6 (0.5 A g^{-1})	88% (200 cycles)	
	244 (1 A g^{-1})	52.1% (1000 cycles)	

References

1 S. Grimme and J. Comput. *Chem.*, 2006, **27**, 1787–1799.

2 J. P. Perdew, K. Burke and M. Ernzerhof, *Phys. Rev. Lett.*, 1996, **77**, 3865.

3 S. J. Clark, M. D. Segall, C. J. Pickard, P. J. Hasnip, M. I. J. Probert, K. Refson and M. C. Payne, *Z. Kristallogr. - Cryst. Mater.*, 2005, **220**, 567–570.

4 X. L. Xiao, L. Zhang, W. L. Xin, M. Yang, Y. H. Geng, M. F. Niu, H. Zhang and Z. Q. Zhu, *Small*, 2024, **20**, 2309271.

5 W. Zhao, J. Fee, H. Khanna, S. March, N. Nisly, S. J. B. Rubio, C. Cui, Z. Li and S. L. Sui, *J. Meter. Chem. A*, 2022, **10**, 6762–6771.

6 R. G. Zhang, P. Liang, H. H. Min, M. M. Niu, S. Y. Jin, Y. T. Jiang, Z. G. Pan, J. X. Yan, X. D. Shen and J. Wang, *Chem. Eng. J.*, 2022, **433**, 133687.

7 M. X. Li, C. Liu, J. M. Meng, P. Hei, Y. Sai, W. J. Li, J. Wang, W. B. Cui, Y. Song and X. -X. Liu, *Adv. Funct. Mater.*, 2024, **34**, 2405659.

8 Q. Chen, X. Lou, Y. F. Yuan, K. You, C. H. Li, C. H. Jiang, Y. Q. Zeng, S. Zhou, J. L. Zhang, G. Y. Hou, J. Lu and Y. P. Tang, *Adv. Mater.*, 2023, **35**, 2306294.

9 Y. N. Zhang, Y. P. Liu, Z. H. Liu, X. G. Wu, Y. X. Wen, H. D. Chen, X. Ni, G. H. Liu, J. J. Huang and S. L. Peng, *J. Energy Chem.*, 2022, **64**, 23–32.

10 W. T. Qu, Y. Cai, B. H. Chen and M. Zhang, *Energy Environ. Mater.*, 2023, **7**, e12645.

11 J. C. Chen, L. Liao, B. Sun, X. Song, M. S. Wang, B. S. Guo, Z. Y. Ma, B. Yu and X. Li, *J. Alloys Compd.*, 2022, **903**, 163833.

12 B. Z. Yu, L. L. Lu, Y. T. He, X. Dai, Y. Wang, T. Wang, S. K. Chong, L. T. Liu, Y. N. Liu and Q. Tan, *J. Colloid Interface Sci.*, 2024, **654**, 56–65.

13 Y. Han, Q. Wu, S. Q. Li, Q. W. Ding, Y. Cao, Y. Y. Gao, R. M. Liu, T. Wang, Z. L. Tian and C. Yang, *J. Alloys Compd.*, 2023, **938**, 168555.

14 Y. H. Liu, Y. D. Ma, Y. Zhang, Y. Li, J. Chen, L. Wang, S. J. Bao, Y. R. Qi, H. Chen and M. W. Xu, *Adv. Energy Mater.*, 2024, **14**, 2304161.

15 S. J. Luo, J. Xu, B. H. Yuan, L. Xu, R. Zheng, Y. S. Wang, M. J. Zhang, Y. Lu and Y. S. Luo, *Carbon*, 2023, **203**, 326–336.